RT-PCR to confirm the presence of not only plus-sense RNA (Fig. 3C), but also of minus-sense RNA (data not shown). The band at the expected size was amplified in RT-PCR product for minus-sense RNA, however, it was difficult to compare the quantities from PCR bands (data not shown).

We didn't confirm the possibility of integration of replicon DNA into host genome. However, several reasons were considerable to rule out this possibility. Firstly, replicon RNA, not contaminated with DNA, was transfected into BHK cells in this study. Secondly, replicons didn't contain any integration sequences. Finally, there is no reliable evidence exhibiting integration of flavivirus genome into host cell chromosomes. Therefore, it is unlikely to be integrated in transfected cells.

The G418-resistant cells transfected with Oshima REP-Neo seemed to harbor replication complex persistently, although replication of the replicon RNA was at low level. A replication complex consists of components with NS proteins, unknown cellular proteins and replicating RNAs. It was shown that replication of the virus with defective NS proteins was compensated when the virus was infected in sub-genomic replicon expressing cells [18, 20, 21, 22, 28]. Therefore, the established cells expressing TBEV sub-genomic replicon should be useful for *trans*-complementation analysis to define the amino acid or nucleotide position required for TBEV replication.

Sub-genomic replicon system is also useful tool to study such as assembly and packaging [19, 21], developing of vaccine and delivering system of foreign genes. Sub-genomic replicons have an advantage to separate replication events from assembly and packaging events compared with full-length infectious clone.

TBEV sub-genomic replicon constructed in this study could express reporter gene such as GFP and neo gene. Therefore, the replicon-based expression of foreign genes will be valuable as a vector or vaccine to express and deliver the genes together with packaging systems.

Acknowledgments

This work was supported by the Grant-in-Aid for Scientific Research (B) (No. 13575029), (A) (No. 14206036) and (No. 15780196), the Grant-in-Aid for JSPS Fellows (No. 0012) from the Ministry of Education, Culture, Sports, Science and Technology of Japan, and Health Sciences Grants for Research on Emerging and Re-emerging Infectious Disease from The Ministry of Health, Labour and Welfare of Japan.

References

1. Agapov EV, Frolov I, Lindenbach BD, Pragai BM, Schlesinger S, Rice CM (1998) Noncytopathic Sindbis virus RNA vectors for heterologous gene expression. Proc Natl Acad Sci 95: 12989–12994
2. Behrens SE, Grassmann CW, Thiel HJ, Meyers G, Tautz N (1998) Characterization of an autonomous subgenomic pestivirus RNA replicon. J Virol 72: 2364–2372

3. Blight KJ, Kolykhalov AA, Rice CM (2000) Efficient initiation of HCV RNA replication in cell culture. Science 290: 1972–1974
4. Campbell MS, Pletnev AG (2000) Infectious cDNA clones of Langat tick-borne flavivirus that differ from their parent in peripheral neurovirulence. Virology 269: 225–237
5. Chambers TJ, Hahn CS, Galler R, Rice CM (1990) Flavivirus genome organization, expression, replication. Ann Rev Microbiol 44: 649–688
6. Corver J, Lenches E, Smith K, Robison RA, Sando T, Strauss EG, Strauss JH (2003) Fine mapping of a cis-acting sequence element in yellow fever virus RNA that is required for RNA replication and cyclization. J Virol 77: 2265–2270
7. Dumpis U, Crook D, Oksi J (1999) Tick-borne encephalitis. Clin Infect Dis 28: 882–890
8. Gaunt MW, Sall AA, Lamballerie Xd, Falconar AK, Dzhivanian TI, Gould EA (2001) Phylogenetic relationships of flaviviruses correlate with their epidemiology, disease association and biogeography. J Gen Virol 82: 1867–1876
9. Goto A, Hayasaka D, Yoshii K, Mizutani T, Kariwa H, Takashima I (2002) Genetic and biological comparison of tick-borne encephalitis viruses from Hokkaido and Far-Eastern Russia. Jpn J Vet Res 49: 297–307
10. Gritsun TS, Lashkevich VA, Gould EA (2003) Tick-borne encephalitis. Antiviral Res 57: 129–146
11. Hagino-Yamagishi K, Nomoto A (1989) In vitro construction of poliovirus defective interfering particles. J Virol 63: 5386–5392
12. Haglund M, Gunther G (2003) Tick-borne encephalitis-pathogenesis, clinical course and long-term follow-up. Vaccine 21 Suppl 1: S11–18
13. Hayasaka D, Suzuki Y, Kariwa H, Ivanov L, Volkov V, Demenev V, Mizutani T, Gojobori T, Takashima I (1999) Phylogenetic and virulence analysis of tick-borne encephalitis viruses from Japan and far-eastern Russia. J Gen Virol 80: 3127–3135
14. Hayasaka D, Ivanov L, Leonova GN, Goto A, Yoshii K, Mizutani T, Kariwa H, Takashima I (2001) Distribution and characterization of tick-borne encephalitis viruses from Siberia and far-eastern Asia. J Gen Virol 82: 1319–1328
15. Iacono-Connors LC, Schmaljohn CS (1992) Cloning and sequence analysis of the genes encoding the nonstructural proteins of Langat virus and comparative analysis with other flaviviruses. Virology 188: 875–880
16. Kaplan G, Racaniello VR (1988) Construction and characterization of poliovirus subgenomic replicons. J Virol 62: 1687–1696
17. Khromykh AA, Westaway EG (1997) Subgenomic replicons of the flavivirus Kunjin: construction and applications. J Virol 71: 1497–1505
18. Khromykh AA, Kenney MT, Westaway EG (1998) *trans*-Complementation of flavivirus RNA polymerase gene NS5 by using Kunjin virus replicon-expressing BHK cells. J Virol 72: 7270–7279
19. Khromykh AA, Varnavski AN, Westaway EG (1998) Encapsidation of the flavivirus kunjin replicon RNA by using a complementation system providing Kunjin virus structural proteins in trans. J Virol 72: 5967–5977
20. Khromykh AA, Sedlak PL, Guyatt KJ, Hall RA, Westaway EG (1999) Efficient trans-complementation of the flavivirus kunjin NS5 protein but not of the NS1 protein requires its coexpression with other components of the viral replicase. J Virol 73: 10272–10280
21. Khromykh AA, Sedlak PL, Westaway EG (1999) *trans*-Complementation analysis of the flavivirus Kunjin ns5 gene reveals an essential role for translation of its N-terminal half in RNA replication. J Virol 73: 9247–9255
22. Khromykh AA, Sedlak PL, Westaway EG (2000) *cis*- and *trans*-acting elements in flavivirus RNA replication. J Virol 74: 3253–3263

23. Khromykh AA, Meka H, Guyatt KJ, Westaway EG (2001) Essential role of cyclization sequences in flavivirus RNA replication. J Virol 75: 6719–6728
24. Khromykh AA, Varnavski AN, Sedlak PL, Westaway EG (2001) Coupling between replication and packaging of flavivirus RNA: evidence derived from the use of DNA-basedfull-length cDNA clones of Kunjin virus. J Virol 75: 4633–4640
25. Kuno G, Chang GJ, Tsuchiya KR, Karabatsos N, Cropp CB (1998) Phylogeny of the genus *Flavivirus*. J Virol 72: 73–83
26. Liljestrom P, Garoff H (1991) A new generation of animal cell expression vectors based on the Semliki Forest virus replicon. Biotechnology 9: 1356–1361
27. Indenbach SD, Rice CM (2001) *Flaviviridae*: The viruses and their replication. In: Knipe DM, Howley PM (4th ed) Fields Virology. Lippincott Williams & Wilkins, Philadelphia, pp. 991–1041
28. Liu WJ, Sedlak PL, Kondratieva N, Khromykh AA (2002) Complementation analysis of the flavivirus Kunjin NS3 and NS5 proteins defines the minimal regions essential for formation of a replication complex and shows a requirement of NS3 in cis for virus assembly. J Virol 76: 10766–10775
29. Lohmann V, Korner F, Koch J, Herian U, Theilmann L, Bartenschlager R (1999) Replication of subgenomic hepatitis C virus RNAs in a hepatoma cell line. Science 285: 110–113
30. Mandl CW, Iacono-Connors L, Wallner G, Holzmann H, Kunz C, Heinz FX (1991) Sequence of the genes encoding the structural proteins of the low-virulence tick-borne flaviviruses Langat 21 and Yelantsev. Virology 185: 891–895
31. McKnight KL, Lemon SM (1996) Capsid coding sequence is required for efficient replication of human rhinovirus 14 RNA. J Virol 70: 1941–1952
32. Pang X, Zhang M, Dayton AI (2001) Development of Dengue virus type 2 replicons capable of prolonged expression in host cells. BMC Microbiol 1: 18
33. Pushko P, Parker M, Ludwig GV, Davis NL, Johnston RE, Smith JF (1997) Replicon-helper systems from attenuated Venezuelan equine encephalitis virus: expression of heterologous genes in vitro and immunization against heterologous pathogens in vivo. Virology 239: 389–401
34. Shi PY, Tilgner M, Lo MK (2002) Construction and characterization of subgenomic replicons of New York strain of West Nile virus. Virology 296: 219–233
35. Suss J (2003) Epidemiology and ecology of TBE relevant to the production of effective vaccines. Vaccine 21 Suppl 1, S19–35
36. Takashima I, Morita K, Chiba M, Hayasaka D, Sato T, Takezawa C, Igarashi A, Kariwa H, Yoshimatsu K, Arikawa J, Hashimoto N (1997) A case of tick-borne encephalitis in Japan and isolation of the virus. J Clin Microbiol 35: 1943–1947
37. Takeda T, Ito T, Osada M, Takahashi K, Takashima I (1999) Isolation of tick-borne encephalitis virus from wild rodents and a seroepizootiologic survey in Hokkaido, Japan. Am J Trop Med Hyg 60: 287–291
38. Tzeng WP, Chen MH, Derdeyn CA, Frey TK (2001) Rubella virus DI RNAs and replicons: requirement for nonstructural proteins acting in cis for amplification by helper virus. Virology 289: 63–73
39. Wallner G, Mandl CW, Kunz C, Heinz FX (1995) The flavivirus 3′-noncoding region: extensive size heterogeneity independent of evolutionary relationships among strains of tick-borne encephalitis virus. Virology 213: 169–178
40. Xiong C, Levis R, Shen P, Schlesinger S, Rice CM, Huang HV (1989) Sindbis virus: an efficient, broad host range vector for gene expression in animal cells. Science 243: 1188–1191

41. Varnavski AN, Khromykh AA (1999) Noncytopathic flavivirus replicon RNA-based system for expression and delivery of heterologous genes. Virology 255: 366–375
42. Varnavski AN, Young PR, Khromykh AA (2000) Stable high-level expression of heterologous genes in vitro and in vivo by noncytopathic DNA-based Kunjin virus replicon vectors. J Virol 74: 4394–4403

Author's address: Takuya Iwasaki, Division of Clinical Investigation, Institute of Tropical Medicine, Nagasaki University 1-12-4 Sakamoto, Nagasaki 852-8523, Japan; e-mail: tiwasaki@net.nagasaki-u.oc.jp

Available online at www.sciencedirect.com
SCIENCE DIRECT
Virology 322 (2004) 318–327
VIROLOGY
www.elsevier.com/locate/yviro

A new model of Hantaan virus persistence in mice: the balance between HTNV infection and CD8$^+$ T-cell responses

Koichi Araki,[a] Kumiko Yoshimatsu,[b] Byoung-Hee Lee,[b] Hiroaki Kariwa,[a] Ikuo Takashima,[a] and Jiro Arikawa[b,*]

[a] *Laboratory of Public Health, Department of Environmental Veterinary Sciences, Graduate School of Veterinary Medicine, Hokkaido University, Sapporo 060-0818, Japan*
[b] *Institute for Animal Experimentation, Graduate School of Medicine, Hokkaido University, Sapporo 060-0863, Japan*

Received 25 October 2003; returned to author for revision 10 December 2003; accepted 30 January 2004

Abstract

We established a viral persistence model that involves the adoptive transfer of spleen cells from immunocompetent mice (H-2^d) into Hantaan virus (HTNV)-infected severe combined immunodeficient (SCID, H-2^d) mice. The infection is maintained despite the presence of neutralizing antibodies, without apparent signs of disease, and there is a correlation between HTNV persistence and the lack of HTNV-specific CD8$^+$ T cells. In addition, disseminated HTNV infection before the initiation of immune responses appears to be important for virus persistence. The suppression of HTNV-specific CD8$^+$ T cells in the present model appears to occur at the periphery. The present study also demonstrates that CD8$^+$ T cells contribute to the clearance of HTNV. Thus, it seems that HTNV-specific CD8$^+$ T cells play a key role in HTNV persistence in mice. This model of viral persistence is useful for studies of immune responses and immunocytotherapy against viral infection.

Keywords: Hantaan virus; Hantavirus; SCID mice; Persistent infection; CD8$^+$ T cell; Adoptive transfer

Introduction

Hemorrhagic fever with renal syndrome (HFRS) and hantavirus pulmonary syndrome (HPS) are rodent viral zoonoses that are caused by viruses of the genus *Hantavirus*, family *Bunyaviridae* (Schmaljohn and Hjelle, 1997). At least 22 virus species have been identified (Elliott et al., 2000), which are maintained by natural rodent reservoirs despite the presence of neutralizing antibodies (Meyer and Schmaljohn, 2000). In addition, persistent hantavirus infection in natural rodent reservoirs is established during adulthood without any signs of disease (Meyer and Schmaljohn, 2000). In addition, distinct hantaviruses are associated with a single rodent species (Meyer and Schmaljohn, 2000).

To date, hantaviruses have not been found in the natural host, which is *Mus musculus* (mouse). Although Hantaan virus (HTNV), which is the prototype of the genus *Hantavirus*, is maintained in the rodent species *Apodemus agrarius* in nature (Meyer and Schmaljohn, 2000), it produces a transient infection in adult mice and lethal infection in newborn mice, following experimental infection. Therefore, studies on HTNV using experimental mice have focused on vaccine development (Choi et al., 2003) and the mechanism of viral pathogenicity (Ebihara et al., 2000; Kikuchi et al., 1998; Kim and McKee, 1985; McKee et al., 1985; Yoo et al., 1993). Previously, we established persistent HTNV infection in newborn mice by inoculation of a sublethal dose of HTNV within 24 h of birth (Araki et al., 2003). These findings suggest that the persistently HTNV-infected mouse has potential as a model of persistent viral infections, such as those caused by the human immunodeficiency virus, Epstein–Barr virus, and hepatitis B and C viruses. Persistent HTNV infection in adult mice that were infected as newborns was maintained despite the presence of high-titer neutralizing antibodies (Araki et al.,

* Corresponding author. Institute for Animal Experimentation, Graduate School of Medicine, Hokkaido University, Kita-15, Nishi-7, Sapporo 060-8638, Japan. Fax: +81-11-706-7879.
E-mail address: j_arika@med.hokudai.ac.jp (J. Arikawa).

0042-6822/$ - see front matter © 2004 Elsevier Inc. All rights reserved.
doi:10.1016/j.virol.2004.01.030

2003). However, we were unable to obtain unambiguous evidence that $CD8^+$ T cells contributed to the clearance of HTNV in the previous study (Araki et al., 2003) due to difficulties in modulating the immune responses of newborn mice. Therefore, a more detailed investigation of the mechanism of HTNV persistence requires a new model, that is, one in which the immune responses can be readily controlled and evaluated. In addition, the mouse model of HTNV persistence should provide information regarding the mechanism of persistent hantavirus infection in natural rodent reservoirs.

The mechanism that has been advanced for persistent lymphocytic choriomeningitis virus (LCMV) infection provides a useful platform for the evaluation of our model of HTNV persistence because cytopathic effects are either absent or incomplete in both LCMV- (Borrow and Oldstone, 1997) and HTNV-infected cells (Pensiero et al., 1992; Yanagihara and Silverman, 1990). In LCMV-infected adult mice, high-level viral replication and disseminated infection of the organs and tissues are important for the establishment of persistent infection that is accompanied by the absence of virus-specific $CD8^+$ T cells (Borrow and Oldstone, 1997). Therefore, to establish the new model of HTNV persistence, we hypothesized that high-level HTNV replication and disseminated infection of organs and tissues in mice might facilitate persistent HTNV infection that is associated with the absence of HTNV-specific $CD8^+$ T cells.

In the present study, we investigated the above-described hypothesis. We succeeded in establishing a new model of viral persistence that involves the adoptive transfer of spleen cells into severe combined immunodeficient (SCID) mice 14 days after HTNV infection. The mechanism of HTNV persistence in these mice was examined and is the basis of this report.

Results

Adoptive transfer of spleen cells to HTNV-infected SCID mice

Infection of adult SCID mice with HTNV leads to disseminated infection. In efforts to investigate whether disseminated HTNV infection before the induction of immune responses affected persistent infection, we performed the adoptive transfer of syngeneic adult immunocompetent spleen cells to HTNV-infected SCID mice, as illustrated in Fig. 1. First, we examined the spread of HTNV infection in SCID mice before the adoptive transfer of spleen cells by measuring the levels of N protein in each organ (Fig. 2). On day 7 after virus infection, N protein was detected only in the spleens. Disseminated infection was observed in various organs (except for the brain) on day 14 postinfection. On day 21 postinfection, the N protein was detected in all of the tissues examined, including the brain. The largest accumulation of N protein was found in the lungs. We then carried out the adoptive transfer of spleen cells from uninfected immunocompetent BALB/c mice into HTNV-infected, MHC-identical SCID mice (Table 1). These SCID mice, which were the recipients of immunocompetent syngeneic spleen cells on days 0, 7, 14, and 21 after virus infection, all survived (Table 1). Although the SCID mice that received syngeneic cells

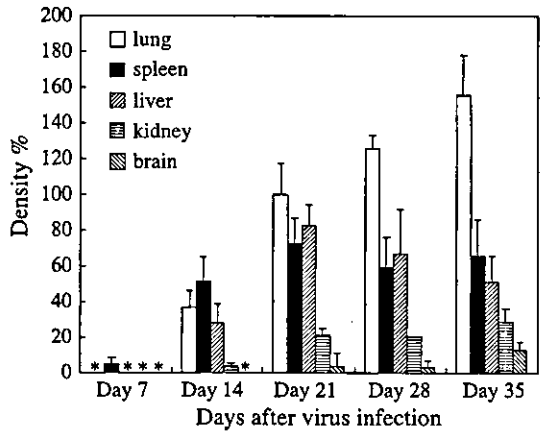

Fig. 2. Measurement of N protein levels in the organs of the HTNV-infected SCID mice. Four SCID mice per group were inoculated intraperitoneally with 2400 FFU HTNV. On days 7, 14, 21, 28, and 35 after virus infection, the lungs, spleens, livers, kidneys, and brains were obtained from the HTNV-infected SCID mice. The amount of N protein in each organ was measured by Western blotting. Band density was determined by the NIH Image 1.63 analysis software. To calculate the density of each point, the average density of the lungs of the SCID mice at day 21 after virus infection was set at 100%. The asterisks indicate that no band was detected. These results were obtained in two independent experiments. The bars represent the SD of the mean for each organ.

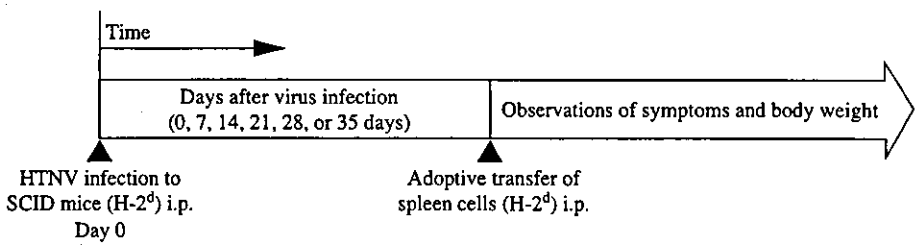

Fig. 1. Experimental design for the adoptive transfer of spleen cells. SCID mice ($H\text{-}2^d$) that were inoculated intraperitoneally with 2400 FFU of HTNV received 2×10^7 spleen cells from immunocompetent BALB/c mice ($H\text{-}2^d$) at the indicated times after virus infection. The condition of the SCID mice was observed.

Table 1
Adoptive transfer of spleen cells into SCID mice

HTNV infection before spleen cell transfer[a]	Spleen cell transfer[b] (day postinfection of transfer)	No. of mice Survivors/ tested	Time to death (days)	Outward symptoms[c]
+	+ (day 0)	4/4	–	–
+	+ (day 7)	4/4	–	–
+	+ (day 14)	4/4	–	–
+	+ (day 21)	4/4	–	+
+	+ (day 28)	2/4	44, 44	+
+	+ (day 35)	0/4	41, 44, 46, 51	+
–	+	4/4	–	–
+	–	0/4	38, 44, 46, 46	+

[a] SCID mice (H-2^d) were inoculated (+) intraperitoneally with HTNV (2400 FFU) or uninfected (–).
[b] The SCID mice either received 2×10^7 spleen cells intraperitoneally from immunocompetent (H-2^d) mice (+) or did not undergo adoptive transfer (–).
[c] Waddling gait and ruffled fur symptoms.

on days 0, 7, and 14 postinfection showed no apparent symptoms, those that received cells on day 21 demonstrated waddling gait and ruffled fur symptoms (Table 1). As shown in Table 1, 2/4 mice that received syngeneic spleen cells on day 28 and 4/4 mice that received syngeneic spleen cells on day 35 died at various time points thereafter, which suggests that the adoptive transfer of spleen cells by day 21 postinfection with HTNV is critical for survival. The body weights of the SCID mice that received spleen cells on days 0, 7, 14, and 21 postinfection were measured and compared with those of the SCID controls (no adoptive transfer after virus infection) (data not shown). The body weights of the control mice decreased from day 21 after virus infection. Mice that received splenocytes on days 0 and 7 after virus infection showed no decrease in body weight after adoptive transfer (data not shown). Although the SCID mice that received spleen cells on day 14 after virus infection showed some weight loss on day 9 after adoptive transfer (data not shown), they returned to their normal body weight shortly thereafter. On the other hand, mice that received splenocytes on day 21 after virus infection showed marked body weight loss and took a long time to return to normal body weight (data not shown). In subsequent experiments, to investigate the relationship between disseminated HTNV infection before the induction of immune responses and HTNV persistence in apparently asymptomatic SCID mice following adoptive transfer of spleen cells, we used SCID mice into which spleen cells had been transferred on days 0 and 14 after virus infection.

HTNV-specific immune responses and N protein levels in SCID mice that received spleen cells on days 0 and 14 after virus infection

Previously, we established an assay for determining the frequency of HTNV-specific CD8$^+$ T cells using intracellular gamma interferon (IFN-γ) detection (Araki et al., 2003). Using this method, HTNV-specific CD8$^+$ T-cell responses were measured on day 30 post-transfer in SCID mice that had received spleen cells by adoptive transfer on days 0 and 14 after virus infection (Fig. 3A). All of the mice that had undergone adoptive transfer on day 0 after virus infection retained HTNV-specific CD8$^+$ T cells (Fig. 3A, left panel). In contrast, HTNV-specific CD8$^+$ T cells were not detected in SCID mice that had undergone adoptive transfer on day 14 after virus infection (Fig. 3A, right panel). These results suggest that disseminated HTNV infection suppresses the induction of HTNV-specific CD8$^+$ T cells. High neutralizing antibody titers were observed in both groups (Fig. 3A). The levels of N protein were measured in the lungs. Although N protein was not detected in SCID mice that had undergone adoptive transfer on day 0 after virus infection (Fig. 3A, left panel), all of the mice that had undergone adoptive transfer on day 14 after virus infection carried N protein in their lungs (Fig. 3A, right panel). Thus, SCID mice that had received spleen cells on day 14 after virus infection showed persistent infection despite the presence of neutralizing antibodies. This SCID mouse model of persistent HTNV infection suggests that the lack of HTNV-specific CD8$^+$ T cells is important for viral persistence. These data indicate that persistent infection is possible in mice that display disseminated HTNV infection before the induction of immune responses.

Kinetics of HTNV-specific immune responses and the levels of N protein in SCID mice that had received spleen cells by adoptive transfer on day 14 after virus infection

We examined the kinetics of the HTNV-specific immune responses and the levels of N protein in SCID mice that had undergone adoptive transfer on day 14 after virus infection (Fig. 3B). On day 60 after adoptive transfer, all of the mice had N protein in their lungs and lacked HTNV-specific CD8$^+$ T cells (Fig. 3B, left panel). On day 90 after adoptive transfer, HTNV-specific CD8$^+$ T cells had appeared in 1/4 of the mice, and this was accompanied by low levels of N protein (Fig. 3B, center panel). On day 120 after adoptive transfer, the number of mice that had HTNV-specific CD8$^+$ T cells had increased, and these mice had undetectable levels of N protein in their lungs (Fig. 3B, right panel). However, even at day 120 after adoptive transfer, 1/4 of the mice continued to have N protein in the lungs and lacked HTNV-specific CD8$^+$ T cells (Fig. 3B, right panel). On the other hand, high neutralizing antibody titers were observed in all of these mice (Fig. 3B). In addition, we measured the tumor necrosis factor-alpha (TNF-α) production of the IFN-γ-producing cells upon co-culture with HTNV-infected P388D1 cells. The HTNV-specific CD8$^+$ T-cell populations in the SCID mice that had received spleen cells on days 0 and 14 after virus infection contained a significant percentage (approximately

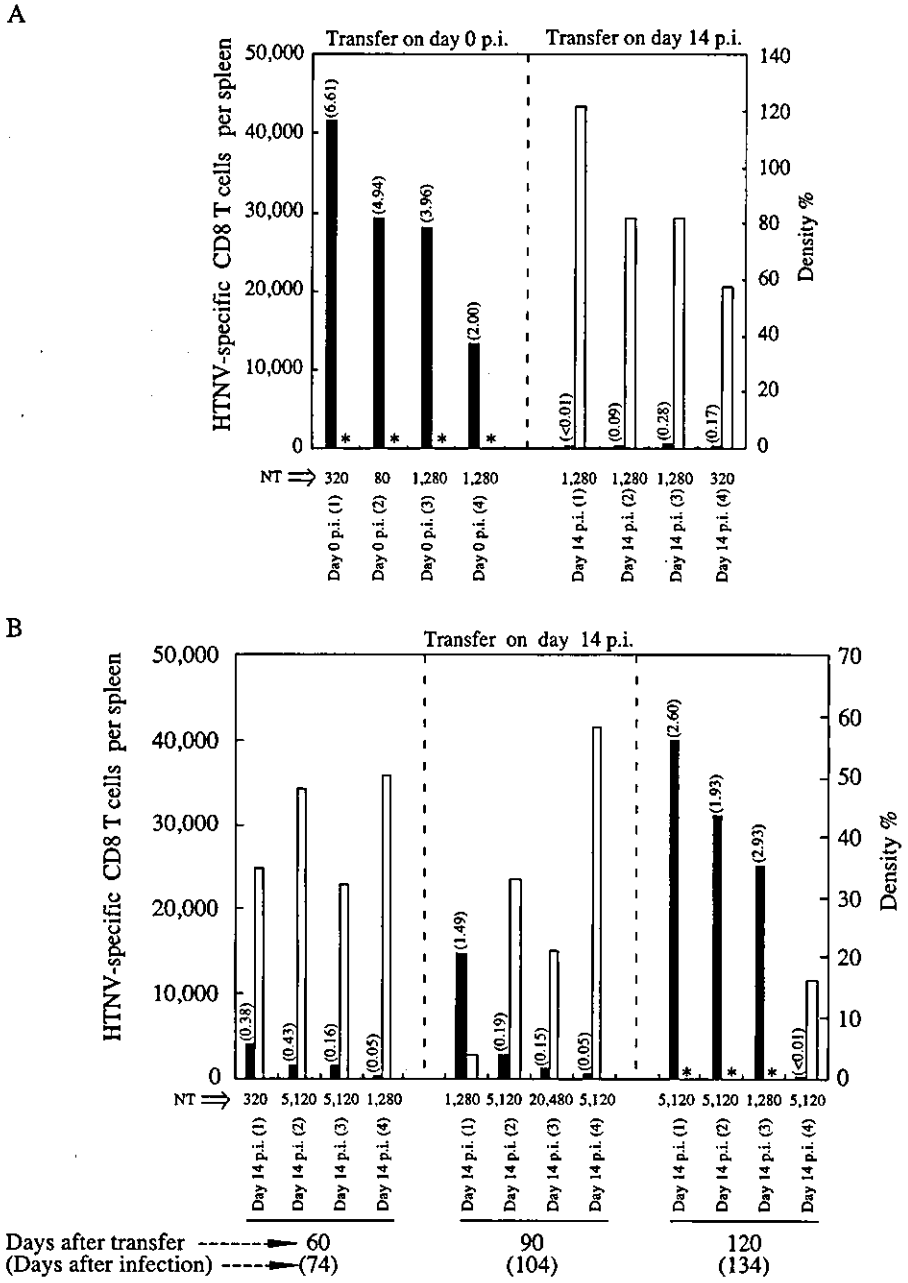

Fig. 3. Measurements of N protein levels in the lungs, neutralizing antibody titers (NT) in the sera, and IFN-γ-producing, HTNV-specific $CD8^+$ T-cell responses in SCID mice, following adoptive transfer of spleen cells on days 0 or 14 after virus infection. SCID mice were inoculated intraperitoneally with 2400 FFU of HTNV. On days 0 or 14 postinfection (p.i.), 2×10^7 spleen cells from immunocompetent mice were adoptively transferred into the HTNV-infected SCID mice. (A) On day 30 after the adoptive transfer, the lungs, sera, and spleens were removed from the SCID mice that received spleen cells on days 0 (A left) or 14 (A right) after virus infection. (B) On days 60 (B left), 90 (B center), and 120 (B right) after adoptive transfer, the lungs, sera, and spleens were removed from the SCID mice that received spleen cells on day 14 after virus infection. The black bars represent the numbers of HTNV-specific $CD8^+$ T cells that produced IFN-γ, and the white bars represent the levels of N protein. To detect HTNV-specific $CD8^+$ T cells, spleen cells and HTNV-infected P388D1 cells were co-cultured at a ratio of 1:0.5 in the presence of brefeldin A and IL-2. After a 6-h incubation, IFN-γ-producing $CD8^+$ T cells were detected by flow cytometry. The data are shown as the number of IFN-γ-producing HTNV-specific $CD8^+$ T cells per spleen. No $CD8^+$ IFN-γ^+ cells were detected from the combination of spleen cells and uninfected P388D1 cells (data not shown). The values above the black bars are the percentages of IFN-γ^+ cells among $CD8^+$ T cells. The levels of N protein in the lungs were measured by Western blotting. The band densities were determined using the NIH Image 1.63 analysis software. To calculate the density of each mouse lung, the average density of the HTNV-infected SCID mouse lung on day 21 after virus infection was set at 100%, as described in the legend to Fig. 2. The asterisks indicate where no band was detected. FRNTs were carried out using sera. The neutralizing antibody titer is expressed as the reciprocal of the highest serum dilution that resulted in a reduction of >80% in the number of infected cell foci. Uninfected SCID mice that received spleen cells lacked HTNV-specific $CD8^+$ T cells, N protein in the lungs, and neutralizing antibodies (data not shown). These results were obtained in two independent experiments.

4%) of IFN-γ-producing cells, approximately 50% of which also produced TNF-α (Fig. 4). Thus, the HTNV-specific $CD8^+$ T cells of SCID mice that had undergone adoptive transfer on day 14 after virus infection were similar, in terms of cytokine production, to those of SCID mice that had undergone adoptive transfer on day 0 after virus infection.

Detection of naïve $CD8^+$ T cells with specificity for HTNV

HTNV-specific $CD8^+$ T cells were induced in SCID mice within 30 days of the adoptive transfer of spleen cells on day 0 postinfection (Fig. 3A, left panel). Knowledge regarding the origin of these HTNV-specific $CD8^+$ T cells is important for a complete understanding of the mechanism underlying the HTNV-specific $CD8^+$ T-cell suppression that had been induced in SCID mice following adoptive transfer on day 14 after virus infection. To examine whether naïve $CD8^+$ T cells with specificity for HTNV existed in the spleen cells used for adoptive transfer, the spleen cells were transferred to HTNV-infected nude mice that lacked the thymus (Fig. 5). HTNV-specific $CD8^+$ T cells were detected in these nude mice on day 30 after adoptive transfer of the spleen cells. This result shows that naïve $CD8^+$ T cells that are specific for HTNV exist in the splenocytes that are used for adoptive transfer, and that the origin of the HTNV-specific $CD8^+$ T cells that are induced in SCID mice following adoptive transfer at day 0 postinfection is constituted by naïve $CD8^+$ T cells with specificity for HTNV. Furthermore, this result suggests that the suppression of HTNV-specific $CD8^+$ T cells seen in SCID mice that had undergone adoptive transfer on day 14 postinfection was caused at the periphery rather than in the thymus because the thymus induces tolerance during the maturation of pre-T cells, but not mature naïve T cells.

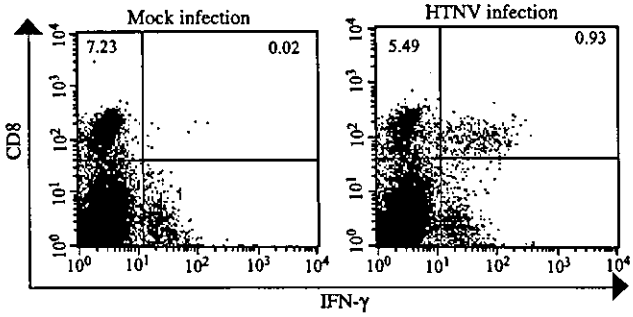

Fig. 5. Detection of naïve $CD8^+$ T cells with specificity for HTNV. Nude mice with either HTNV infection (2400 FFU) or mock infection received 2×10^7 spleen cells from immunocompetent mice on day 0 after virus infection. On day 30 after adoptive transfer, spleen cells were removed from the nude mice. The spleen cells and HTNV-infected P388D1 cells were co-cultured at a ratio of 1:0.5 for 6 h in the presence of brefeldin A and IL-2. IFN-γ-producing, HTNV-specific $CD8^+$ T cells were detected using flow cytometry. The gates were set for spleen cells, and the values shown are the percentages of IFN-γ^- $CD8^+$ and IFN-γ^+ $CD8^+$ T cells. Data from a representative experiment are shown.

$CD8^+$ T cells contribute to HTNV clearance

The results obtained, to date, have shown a correlation between HTNV persistence and the lack of HTNV-specific $CD8^+$ T cells (Fig. 3). To investigate whether $CD8^+$ T cells are required for HTNV clearance, spleen cells from HTNV-immunized immunocompetent BALB/c mice were used for the adoptive transfer (Fig. 6). These spleen cells included many HTNV-specific $CD8^+$ T cells (Fig. 6A). Whole spleen cells or the $CD8^+$ T-cell-depleted spleen cells were adoptively transferred to HTNV-infected SCID mice on day 14 after virus infection. N protein was absent from the lungs of SCID mice that had been the recipients of whole spleen cells, and numerous HTNV-specific $CD8^+$ T cells were detected (Figs. 6B, left panel, and C). In contrast, HTNV persistence was observed in SCID mice that had been

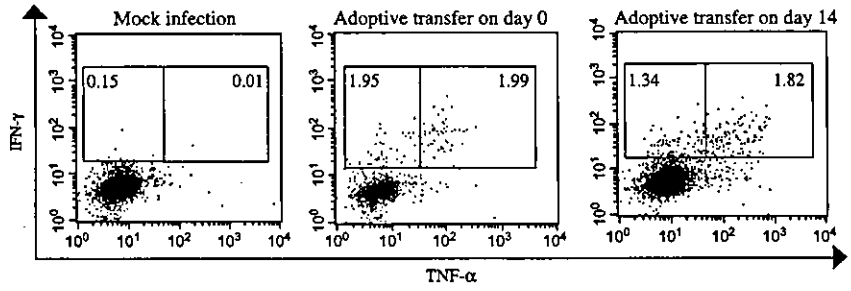

Fig. 4. TNF-α production by IFN-γ-producing $CD8^+$ T cells in splenocytes obtained from the SCID mice that received spleen cells on days 0 or 14 after virus infection. The SCID mice were infected with HTNV (2400 FFU) and received 2×10^7 spleen cells on days 0 or 14 postinfection. On day 30 after the adoptive transfer, spleen cells were obtained from the SCID mice that were adoptively transferred on day 0 postinfection. On day 120 after the adoptive transfer, spleen cells were obtained from the SCID mice that had undergone adoptive transfer on day 14 postinfection. As the control, 2×10^7 spleen cells were transferred into mock-infected SCID mice, and the spleen cells were removed from these mice on day 30 after the adoptive transfer. All of the spleen cells were tested for TNF-α production. To detect TNF-α^+ $CD8^+$ T cells, the spleen cells and HTNV-infected P388D1 cells were co-cultured at a ratio of 1:0.5 for 6 h in the presence of brefeldin A and IL-2. TNF-α production by $CD8^+$ IFN-γ^+ cells was detected using flow cytometry. The gates were set for $CD8^+$ T cells, and the values shown are the percentages of TNF-α^- IFN-γ^+ cells and TNF-α^+ IFN-γ^+ cells among $CD8^+$ T cells. Data from a representative experiment are shown.

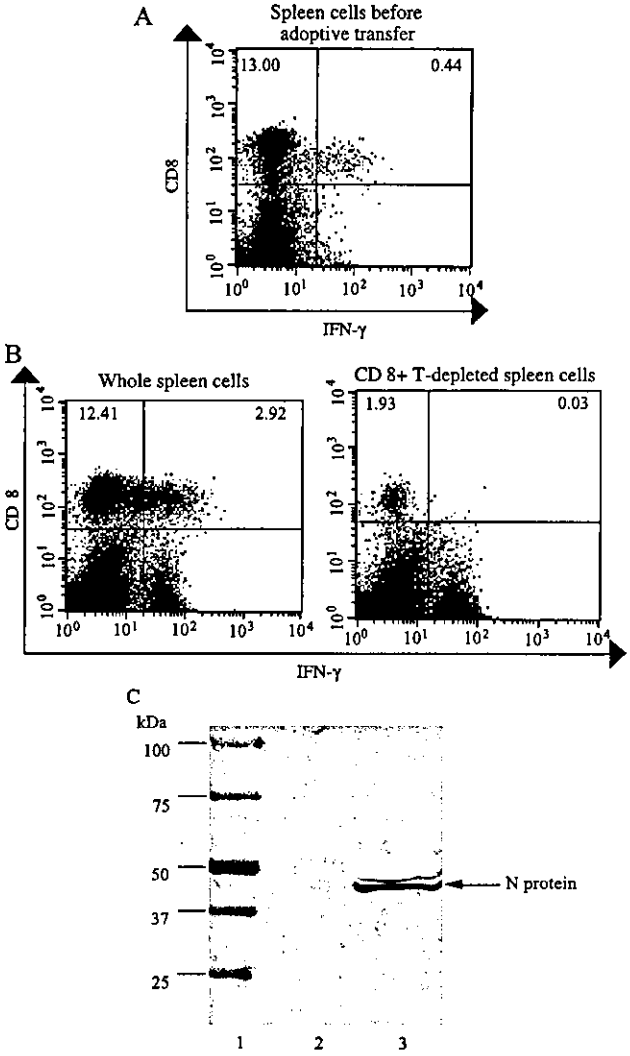

Fig. 6. The contribution of $CD8^+$ T cells to HTNV clearance. Immunocompetent BALB/c mice were inoculated intraperitoneally with 2400 FFU of HTNV. (A) On day 21 after virus infection, spleen cells were removed from the immunocompetent mice. The spleen cells and HTNV-infected P388D1 cells were co-cultured at a ratio of 1:0.5 for 6 h in the presence of brefeldin A and IL-2. IFN-γ-producing, HTNV-specific $CD8^+$ T cells were detected using flow cytometry. The gates were set for spleen cells, and the values shown are the percentages of IFN-γ^- $CD8^+$ and IFN-γ^+ $CD8^+$ T cells. (B and C) Whole spleen cells or $CD8^+$ T-cell-depleted spleen cells (>98% deletion) from the mice in (A) were transferred into SCID mice on day 14 after virus infection. On day 30 after the adoptive transfer, spleen cells and lungs were removed from the SCID mice. The methods described above for (A) were also performed to detect HTNV-specific $CD8^+$ T cells (B). The levels of N protein in the lungs were measured by Western blotting (C). Lane 1, molecular weight marker; lane 2, following the transfer of whole spleen cells; lane 3, following the transfer of $CD8^+$ T-cell-depleted spleen cells. Data from a representative experiment are shown.

recipients of $CD8^+$ T-cell-depleted spleen cells (Fig. 6C). Although the recovery of just a few $CD8^+$ T cells was observed in the SCID mice that had received the $CD8^+$ T-cell-depleted spleen cells, there was a complete absence of HTNV-specific $CD8^+$ T cells in these mice (Fig. 6B, right panel). These data show that $CD8^+$ T cells contribute to the clearance of HTNV.

Discussion

To establish a model of viral persistence in which immune responses could be readily manipulated, we carried out the adoptive transfer of spleen cells into HTNV-infected SCID mice. Persistent HTNV infection was established in SCID mice that had undergone adoptive transfer after disseminated HTNV infection of various organs. This model of viral persistence is characterized by high titers of neutralizing antibodies, no detectable levels of HTNV-specific $CD8^+$ T cells, and no apparent signs of disease. These results suggest that disseminated HTNV infection before the induction of immune responses is important for the establishment of persistent infection and for the suppression of HTNV-specific $CD8^+$ T cells in mice.

We further investigated whether the suppression of HTNV-specific $CD8^+$ T cells occurred in the periphery. Generally, clonal T-cell deletion occurs in the thymus, and there is also evidence for deletion or suppression in the periphery. In the thymus, T cells with specificities for ubiquitous self-antigens are deleted by negative selection during the process of maturation of pre-T cells, which are derived from hematopoietic stem cells (Anderson et al., 1996; Zuniga-Pflucker and Lenardo, 1996). In contrast, anergy or clonal deletion of naïve T cells with specificities for self-antigens that do not exist in the thymus take place in the periphery. Nude mice, which lack the thymus, were used to detect naïve $CD8^+$ T cells with specificity for HTNV in the spleen cells that were used for adoptive transfer. Because the thymus is required for the maturation of pre-T cells that are derived from hematopoietic stem cells, nude mice are unable to make T cells from hematopoietic stem cells or pre-T cells. The nude mice that received spleen cells on day 0 after HTNV infection had significant numbers of HTNV-specific $CD8^+$ T cells (Fig. 5). Consequently, the origin of the HTNV-specific $CD8^+$ T cells that were induced in the nude mice was naïve $CD8^+$ T cells, and not hematopoietic stem cells. These findings suggest that naïve HTNV-specific $CD8^+$ T cells existed in the spleen cells used for adoptive transfer, and that these T cells experienced anergy or clonal deletion in the periphery of SCID mice that had undergone adoptive transfer on day 14 after virus infection. These results also suggest that it is possible to establish persistent HTNV infection, not only in newborn mice that have immature immune systems, as shown previously (Araki et al., 2003), but also in adult mice that possess mature immune systems.

In a previous study of HTNV-infected newborn mice (Araki et al., 2003), we were unable to demonstrate conclusively that $CD8^+$ T cells contributed to HTNV clearance due to difficulties in modulating the immune responses of

the newborn mice. In our present study, HTNV persistence was observed in SCID mice that were recipients of $CD8^+$ T-cell-depleted syngeneic spleen cells, obtained from HTNV-immunized immunocompetent mice. In contrast, SCID mice that were recipients of unfractionated spleen cells from HTNV-immunized mice showed an absence of detectable N protein (Fig. 6). This demonstrates that $CD8^+$ T cells contribute to HTNV clearance. Additionally, it is known that HTNV-specific $CD8^+$ T cells are induced in both HTNV-infected humans and mice (Araki et al., 2003; Park et al., 2000; Van Epps et al., 1999), and that these infections are transient. In addition, hantavirus-specific $CD8^+$ T cells have been observed in other transient hantavirus (Puumala virus and Sin Nombre virus) infections of humans (Ennis et al., 1997; Van Epps et al., 2002). Taken together, it seems that $CD8^+$ T cells are required for the clearance of hantaviruses. These results also suggest that persistent hantavirus infections in natural rodent reservoirs are due to escape from $CD8^+$ T cell immune surveillance, although it is unclear how hantaviruses escape the hantavirus-specific $CD8^+$ T cells in natural rodent reservoirs.

In addition to the mechanism of HTNV clearance, the mechanism of HTNV persistence is a key issue in this mouse model. HTNV-infected SCID mice that did not receive syngeneic spleen cells died from the infection, and HTNV persistence was established in HTNV-infected SCID mice that received $CD8^+$ T-cell-depleted syngeneic spleen cells from HTNV-immunized immunocompetent BALB/c mice. These results indicate that $CD4^+$ T cells and B cells contribute to viral persistence in the absence of any signs of disease.

However, B cells seem to be more important than $CD4^+$ T cells for HTNV persistence in mice. Nude mice showed asymptomatic viral persistence when infected intraperitoneally with HTNV (K. Yoshimatsu, and J. Arikawa, unpublished data). The persistently HTNV-infected nude mice had low titers of HTNV-specific antibodies. These results suggest that the B cells and low-titer antibodies that are induced without $CD4^+$ T-cell help are important for HTNV persistence in mice. $CD4^+$ T cells may simply play a supporting role in the production of high-titer antibodies that are specific for HTNV.

Moreover, it seems that the role of HTNV-specific antibodies that are produced by the B cells in persistently HTNV-infected mice is to evade fatal disease. Generally, the high-level growth of HTNV in the brain is important in producing the fatal outcome in mice (Ebihara et al., 2000; Kurata et al., 1983; McKee et al., 1985). The passive transfer of HTNV-specific antibodies into infected mice confers protection against lethal infection (Arikawa et al., 1992; Yoshimatsu et al., 1993). Therefore, antibodies are important for the suppression of HTNV growth in the brain and in the evasion of fatal illness. These findings suggest that HTNV-specific antibodies are necessary for HTNV persistence in the absence of morbidity. Thus, the existence of B cells is essential for the establishment of persistent HTNV infection without any signs of disease in mice.

Additionally, NK cells are known to contribute to innate defense against viral and bacterial infections. SCID mice have mature NK cells that are phenotypically and functionally indistinguishable from NK cells found in immunocompetent mice (Kumar et al., 1989). However, because the HTNV-infected SCID mice died from the infection, it is clear that NK cells alone are not sufficient to confer protective immunity against HTNV infection. However, it remains unclear whether NK cells act cooperatively with other components of the immune system to generate protective immunity.

The present model of viral persistence is similar, in terms of the presence of neutralizing antibodies and the lack of apparent signs of disease, to natural rodent reservoirs that are persistently infected with hantaviruses (Meyer and Schmaljohn, 2000). Although it is believed that persistent hantavirus infection in natural rodent reservoirs is life-long (Meyer and Schmaljohn, 2000), HTNV was eliminated by day 120 post-transfer from most of the SCID mice that had undergone adoptive transfer on day 14 after virus infection. In this respect, it appears that the present model does not reflect, completely, the natural rodent reservoir. Therefore, comparisons of the HTNV-specific T-cell responses between the present model and the natural rodent reservoir need to be made within the context of these findings, and the results should be important with regard to understanding persistent hantavirus infection in nature. However, this type of comparison is difficult because, to the best of our knowledge, there have been no reports on the T-cell responses in hantavirus-infected natural rodent reservoirs. To further investigate the mechanism of persistent hantavirus infection in natural rodent reservoirs, the establishment of a method for measuring hantavirus-specific $CD8^+$ T cells in natural rodent reservoirs is required.

When the spleen cells were adoptively transferred into HTNV-infected SCID mice on day 21 after virus infection, an exacerbation of disease symptoms was observed, as compared to HTNV-infected SCID mice that did not undergo adoptive transfer. Previously, we showed an increase in the serum BUN levels of HTNV-infected SCID mice following adoptive transfer (Yoshimatsu et al., 1997). These results suggest that immune system-mediated pathogenicity occurred in these mice. In addition, both HFRS and HPS patients demonstrate varying degrees of pathology that are thought to be immune-related because hantaviruses infect endothelial cells without direct cytopathic effects (Pensiero et al., 1992; Sundstrom et al., 2001; Zaki et al., 1995), and this is accompanied by marked increases in both $CD8^+$ T-cell numbers and in the levels of inflammatory cytokines, such as IFN-γ, TNF-α, and IL-6 (Chen and Yang, 1990; Huang et al., 1994; Krakauer et al., 1994; Linderholm et al., 1996; Markotic et al., 1999; Temonen et al., 1996). Therefore, the adoptive transfer on day 21 after virus infection of

SCID mice may have potential as a model of HFRS and HPS.

In summary, we have established a model of viral persistence using SCID mice and HTNV. It seems that disseminated HTNV infection before the induction of immune responses plays a key role in the persistent infection and suppression of the generation of HTNV-specific $CD8^+$ T cells from the naïve $CD8^+$ T cells of mice. Furthermore, we have demonstrated that $CD8^+$ T cells contribute to HTNV clearance. The present model of viral persistence is useful for studies of immune responses and of immunocytotherapy against viral infection because the induction of immune responses, and the types of immunocytes used for adoptive transfer, can be readily manipulated.

Materials and methods

Mice

Six-week-old BALB/c mice ($H\text{-}2^d$) and six-week-old BALB/c-nu/nu mice (nude mice, $H\text{-}2^d$) were obtained from SLC (Hamamatsu, Japan). Six-week-old CB-17/Lcr-scid Jcl mice (SCID mice, $H\text{-}2^d$) were obtained from CLEA Japan (Tokyo, Japan). All of the mice were treated according to the laboratory animal control guidelines of our institute, which conform to those of the U.S. National Institute of Health. All of the experiments were carried out in a class P3 facility.

Viral infection of mice

HTNV cl-1 (Ebihara et al., 2000) was obtained by plaque cloning of HTNV strain 76-118. The virus was propagated in the E6 Vero cell clone (Vero E6), which was grown in Eagle's minimal essential medium (EMEM; Invitrogen) that was supplemented with 5% fetal bovine serum (FBS). Six-week-old adult BALB/c, nude, and SCID mice were inoculated intraperitoneally with 2400 focus-forming units (FFU) of HTNV.

Cell preparations

Single-cell suspensions of spleen cells were obtained by homogenizing spleens through a mesh. The erythrocytes were lysed with 0.83% NH_4Cl. For the adoptive transfer experiments, the spleen cells were suspended in RPMI 1640 medium (Invitrogen) that was supplemented with 10% FBS and 50 μM 2-mercaptoethanol (ME) and incubated in a 150-cm^2 cell culture flask for 2 h at 37 °C in 5% CO_2 to remove adherent cells. To deplete the $CD8^+$ T cells, the spleen cells (1×10^7 cells/ml) were treated with the rat anti-mouse CD8 monoclonal antibody (mAb, 1 μg/ml; Serotec) or rat IgG (isotype control, 1 μg/ml; Serotec) for 1 h on ice, and then incubated in a 1:10 dilution of rabbit complement (Low-Tox-M; Cederlane Laboratories, Hornby, ON, Canada) for 1 h at 37 °C. Flow cytometric analysis was performed to determine the efficacy of the procedure; >98% of the $CD8^+$ T-cell subpopulation was depleted.

Adoptive transfer of spleen cells into SCID or nude mice

Spleen cells were obtained from naïve BALB/c mice or HTNV-infected BALB/c mice, 21 days after infection. The SCID and nude mice received either 2×10^7 spleen cells or 1.7×10^7 $CD8^+$ T-cell-depleted spleen cells by intraperitoneal injection.

Clinical features of the mice

Waddling gait, ruffled fur, weight loss, and mortality were used to evaluate the clinical severity of HTNV infection.

Fluorescence staining and flow cytometry

To detect HTNV-specific $CD8^+$ T cells, we used flow cytometry to assay the intracellular cytokines of $CD8^+$ T cells that were stimulated by HTNV-infected antigen-presenting cells, as described previously (Araki et al., 2003). Briefly, spleen cells were added to 96-well round-bottomed plates at a concentration of 5×10^5 cells/well in RPMI 1640 medium that was supplemented with 10% FBS, 50 μM 2-ME, 20 U/ml recombinant interleukin (IL)-2 (Sigma Co., St. Louis, MO), and 10 μg/ml brefeldin A (Sigma), along with the HTNV-infected or noninfected P388D1 cells at a concentration of 2.5×10^5 cells/well. After a 6-h incubation, the cells were stained with Tri-color (TC)-conjugated rat anti-mouse CD8a (Ly-2) mAb (Caltag Laboratories, San Francisco, CA) for 30 min on ice, then fixed and permeabilized with saponin (Sigma), before the addition of the fluorescein isothiocyanate-conjugated rat anti-mouse IFN-γ mAb (Caltag Laboratories) and the *R*-phycoerythrin-conjugated rat anti-mouse TNF-α mAb (Caltag Laboratories). The cell samples were analyzed using the FACSCalibur system (Becton Dickinson), and the data analyses were conducted with CellQuest (Becton Dickinson).

Western blotting for the detection of N protein in lung, liver, spleen, kidney, and brain tissues of HTNV-infected mice

Western blotting was performed using previously published methods (Yoshimatsu et al., 1995). Briefly, 20 μl of 10% tissue homogenate was used as the antigen. Polyclonal rabbit anti-N protein antibody (diluted 1:800 with PBS) (Araki et al., 2001), which was prepared by immunizing a rabbit with the truncated N protein expressed in *E. coli*, was used to detect the N protein on the membrane. Horseradish peroxidase-conjugated goat anti-rabbit IgG (1:500, Jackson ImmunoResearch, West Grove, PA) was used as the sec-

ondary antibody. Western blotting was quantified by densitometry with the NIH Image v. 1.63 analysis software. NIH Image was developed at the National Institute of Health and is available on the Internet (http://rsb.info.nih.gov/nih-image/).

Focus reduction neutralization test

Focus reduction neutralization tests (FRNTs) were performed using the previously published method (Araki et al., 2001). Briefly, 100 μl of serial 4-fold dilutions of serum that had been heat-inactivated for 30 min at 56 °C were mixed with equal volumes of virus suspensions that contained 400 FFU of HTNV and incubated at 37 °C for 1 h. Then, 50-μl aliquots of the mixture were inoculated onto Vero E6 cell monolayers in 96-well plates and incubated at 37 °C for 1 h in a 5% CO_2 incubator. After adsorption for 1 h, the wells were overlaid with EMEM that contained 1.5% carboxymethyl cellulose. The plates were incubated for 7 days, and the monolayers were fixed with acetone/methanol (1:1) and dried. For the detection of virus foci, the polyclonal rabbit anti-N protein antibody was added to the 96-well plate. The plate was incubated for 1 h at 37 °C, washed with PBS, and then incubated with horseradish peroxidase-conjugated goat anti-rabbit IgG (1:500; Jackson ImmunoResearch) for 1 h at 37 °C. The plate was washed with PBS, and the viral foci were stained with the 3-amino-9-ethylcarbazole substrate (Sigma), according to the manufacturer's instructions.

Acknowledgments

K.A. is a Research Fellow of the Japan Society for the Promotion of Science (JSPS) and was supported by JSPS Research Fellowships for Young Scientists. This work was supported, in part, by Grants-in-Aid for Scientific Research and the Development of Scientific Research from the Ministry of Education, Culture, Sports, Science and Technology, Tokyo, Japan. Textcheck (English language consultants) revised the English in the final draft of the manuscript.

References

Anderson, G., Moore, N.C., Owen, J.J., Jenkinson, E.J., 1996. Cellular interactions in thymocyte development. Annu. Rev. Immunol. 14, 73–99.

Araki, K., Yoshimatsu, K., Ogino, M., Ebihara, H., Lundkvist, A., Kariwa, H., Takashima, I., Arikawa, J., 2001. Truncated hantavirus nucleocapsid proteins for serotyping hantaan, seoul, and dobrava hantavirus infections. J. Clin. Microbiol. 39 (7), 2397–2404.

Araki, K., Yoshimatsu, K., Lee, B.H., Kariwa, H., Takashima, I., Arikawa, J., 2003. Hantavirus-specific CD8(+)-T-cell responses in newborn mice persistently infected with Hantaan virus. J. Virol. 77 (15), 8408–8417.

Arikawa, J., Yao, J.S., Yoshimatsu, K., Takashima, I., Hashimoto, N., 1992. Protective role of antigenic sites on the envelope protein of Hantaan virus defined by monoclonal antibodies. Arch. Virol. 126 (1–4), 271–281.

Borrow, P., Oldstone, M.B.A., 1997. Lymphocytic choriomeningitis virus. In: Nathanson, N. (Ed.), Viral Pathogenesis. Lippincott-Raven, Philadelphia, pp. 593–627.

Chen, L.B., Yang, W.S., 1990. Abnormalities of T cell immunoregulation in hemorrhagic fever with renal syndrome. J. Infect. Dis. 161 (5), 1016–1019.

Choi, Y., Ahn, C.J., Seong, K.M., Jung, M.Y., Ahn, B.Y., 2003. Inactivated Hantaan virus vaccine derived from suspension culture of Vero cells. Vaccine 21 (17–18), 1867–1873.

Ebihara, H., Yoshimatsu, K., Ogino, M., Araki, K., Ami, Y., Kariwa, H., Takashima, I., Li, D., Arikawa, J., 2000. Pathogenicity of Hantaan virus in newborn mice: genetic reassortant study demonstrating that a single amino acid change in glycoprotein G1 is related to virulence. J. Virol. 74 (19), 9245–9255.

Elliott, R.M., Bouloy, M., Calisher, C.H., Goldbach, R., Moyer, J.T., Nichol, S.T., Pettersson, R., Plyusnin, A., Schmaljohn, C.S., 2000. Family *Bunyaviridae*. In: van Regenmortel, M.H.V., Fauquet, C.M., Bishop, D.H.L., Carstens, E.B., Estes, M.K., Lemon, S.M., Maniloff, J., Mayo, M.A., McGeoch, D.J., Pringle, C.R., Wickner, R.B. (Eds.), Virus Taxonomy: Classification and Nomenclature of Viruses. Seventh Report of the International Committee on Taxonomy of Viruses. Academic Press, San Diego, CA, pp. 599–621.

Ennis, F.A., Cruz, J., Spiropoulou, C.F., Waite, D., Peters, C.J., Nichol, S.T., Kariwa, H., Koster, F.T., 1997. Hantavirus pulmonary syndrome: CD8+ and CD4+ cytotoxic T lymphocytes to epitopes on Sin Nombre virus nucleocapsid protein isolated during acute illness. Virology 238 (2), 380–390.

Huang, C., Jin, B., Wang, M., Li, E., Sun, C., 1994. Hemorrhagic fever with renal syndrome: relationship between pathogenesis and cellular immunity. J. Infect. Dis. 169 (4), 868–870.

Kikuchi, M., Yoshimatsu, K., Arikawa, J., Yoshida, R., Yoo, Y.C., Isegawa, Y., Yamanishi, K., Tono-oka, S., Azuma, I., 1998. Characterization of neutralizing monoclonal antibody escape mutants of Hantaan virus 76118. Arch. Virol. 143 (1), 73–83.

Kim, G.R., McKee Jr., K.T., 1985. Pathogenesis of Hantaan virus infection in suckling mice: clinical, virologic, and serologic observations. Am. J. Trop. Med. Hyg. 34 (2), 388–395.

Krakauer, T., Leduc, J.W., Morrill, J.C., Anderson, A.O., Krakauer, H., 1994. Serum levels of alpha and gamma interferons in hemorrhagic fever with renal syndrome. Viral Immunol. 7 (2), 97–101.

Kumar, V., Hackett Jr., J., Tutt, M.M., Garni-Wagner, B.A., Kuziel, W.A., Tucker, P.W., Bennett, M., 1989. Natural killer cells and their precursors in mice with severe combined immunodeficiency. Curr. Top. Microbiol. Immunol. 152, 47–52.

Kurata, T., Tsai, T.F., Bauer, S.P., McCormick, J.B., 1983. Immunofluorescence studies of disseminated Hantaan virus infection of suckling mice. Infect. Immun. 41 (1), 391–398.

Linderholm, M., Ahlm, C., Settergren, B., Waage, A., Tarnvik, A., 1996. Elevated plasma levels of tumor necrosis factor (TNF)-alpha, soluble TNF receptors, interleukin (IL)-6, and IL-10 in patients with hemorrhagic fever with renal syndrome. J. Infect. Dis. 173 (1), 38–43.

Markotic, A., Dasic, G., Gagro, A., Sabioncello, A., Rabatic, S., Kuzman, I., Zgorelec, R., Smoljan, I., Beus, I., Zupanc, T.A., Dekaris, D., 1999. Role of peripheral blood mononuclear cell (PBMC) phenotype changes in the pathogenesis of haemorrhagic fever with renal syndrome (HFRS). Clin. Exp. Immunol. 115 (2), 329–334.

McKee Jr., K.T., Kim, G.R., Green, D.E., Peters, C.J., 1985. Hantaan virus infection in suckling mice: virologic and pathologic correlates. J. Med. Virol. 17 (2), 107–117.

Meyer, B.J., Schmaljohn, C.S., 2000. Persistent hantavirus infections: characteristics and mechanisms. Trends Microbiol. 8 (2), 61–67.

Park, J.M., Cho, S.Y., Hwang, Y.K., Um, S.H., Kim, W.J., Cheong, H.S., Byun, S.M., 2000. Identification of H-2K(b)-restricted T-cell epitopes within the nucleocapsid protein of Hantaan virus and establishment of cytotoxic T-cell clones. J. Med. Virol. 60 (2), 189–199.

Pensiero, M.N., Sharefkin, J.B., Dieffenbach, C.W., Hay, J., 1992. Hantaan virus infection of human endothelial cells. J. Virol. 66 (10), 5929–5936.

Schmaljohn, C., Hjelle, B., 1997. Hantaviruses—A global disease problem. Emerg. Infect. Dis. 3 (2), 95–104.

Sundstrom, J.B., McMullan, L.K., Spiropoulou, C.F., Hooper, W.C., Ansari, A.A., Peters, C.J., Rollin, P.E., 2001. Hantavirus infection induces the expression of RANTES and IP-10 without causing increased permeability in human lung microvascular endothelial cells. J. Virol. 75 (13), 6070–6085.

Temonen, M., Mustonen, J., Helin, H., Pasternack, A., Vaheri, A., Holthofer, H., 1996. Cytokines, adhesion molecules, and cellular infiltration in nephropathia epidemica kidneys: an immunohistochemical study. Clin. Immunol. Immunopathol. 78 (1), 47–55.

Van Epps, H.L., Schmaljohn, C.S., Ennis, F.A., 1999. Human memory cytotoxic T-lymphocyte (CTL) responses to Hantaan virus infection: identification of virus-specific and cross-reactive CD8(+) CTL epitopes on nucleocapsid protein. J. Virol. 73 (7), 5301–5308.

Van Epps, H.L., Terajima, M., Mustonen, J., Arstila, T.P., Corey, E.A., Vaheri, A., Ennis, F.A., 2002. Long-lived memory T lymphocyte responses after hantavirus infection. J. Exp. Med. 196 (5), 579–588.

Yanagihara, R., Silverman, D.J., 1990. Experimental infection of human vascular endothelial cells by pathogenic and nonpathogenic hantaviruses. Arch. Virol. 111 (3–4), 281–286.

Yoo, Y.C., Yoshimatsu, K., Yoshida, R., Tamura, M., Azuma, I., Arikawa, J., 1993. Comparison of virulence between Seoul virus strain SR-11 and Hantaan virus strain 76-118 of hantaviruses in newborn mice. Microbiol. Immunol. 37 (7), 557–562.

Yoshimatsu, K., Yoo, Y.C., Yoshida, R., Ishihara, C., Azuma, I., Arikawa, J., 1993. Protective immunity of Hantaan virus nucleocapsid and envelope protein studied using baculovirus-expressed proteins. Arch. Virol. 130 (3–4), 365–376.

Yoshimatsu, K., Arikawa, J., Yoshida, R., Li, H., Yoo, Y.C., Kariwa, H., Hashimoto, N., Kakinuma, M., Nobunaga, T., Azuma, I., 1995. Production of recombinant hantavirus nucleocapsid protein expressed in silkworm larvae and its use as a diagnostic antigen in detecting antibodies in serum from infected rats. Lab. Anim. Sci. 45 (6), 641–646.

Yoshimatsu, K., Arikawa, J., Ohbora, S., Itakura, C., 1997. Hantavirus infection in SCID mice. J. Vet. Med. Sci. 59 (10), 863–868.

Zaki, S.R., Greer, P.W., Coffield, L.M., Goldsmith, C.S., Nolte, K.B., Foucar, K., Feddersen, R.M., Zumwalt, R.E., Miller, G.L., Khan, A.S., 1995. Hantavirus pulmonary syndrome. Pathogenesis of an emerging infectious disease. Am. J. Pathol. 146 (3), 552–579.

Zuniga-Pflucker, J.C., Lenardo, M.J., 1996. Regulation of thymocyte development from immature progenitors. Curr. Opin. Immunol. 8 (2), 215–224.

Available online at www.sciencedirect.com
SCIENCE DIRECT
Virus Research 101 (2004) 127–134
Virus Research
www.elsevier.com/locate/virusres

Genetic and antigenic characterization of the Amur virus associated with hemorrhagic fever with renal syndrome

Kumari Lokugamage[a], Hiroaki Kariwa[a,*], Nandadeva Lokugamage[a], Hironobu Miyamoto[a], Masahiro Iwasa[a], Tomohiro Hagiya[a], Koichi Araki[a], Atsushi Tachi[a], Tetsuya Mizutani[a], Kumiko Yoshimatsu[b], Jiro Arikawa[b], Ikuo Takashima[a]

[a] *Laboratory of Public Health, Graduate School of Veterinary Medicine, Hokkaido University, Sapporo, Hokkaido 060-0818, Japan*
[b] *Graduate School of Medicine, Hokkaido University, Sapporo, Hokkaido 060-8638, Japan*

Received 6 August 2003; received in revised form 15 December 2003; accepted 19 December 2003

Abstract

The genetic and antigenic characteristics of the Amur (AMR) and Far East (FE) virus lineages, which are both within the genus *Hantavirus*, were studied. Representative viruses, H5 and B78 for AMR and Bao 14 for FE, were used. The entire small (S) and medium (M) segments, except for the 3′- and 5′-ends, were sequenced. The deduced amino acid sequences of AMR had 96.7 and 92.0–92.2% identities with the Hantaan (HTN) virus in the S and M segments, respectively. The amino acid sequences of FE had 99.1 and 97.9% identities in the S and M segments, respectively. The three viral strains and HTN virus had similar binding patterns to a panel of monoclonal antibodies (MAbs), except that one MAb did not bind AMR. However, sera from *Apodemus peninsulae*, naturally infected with AMR virus, neutralized homologous viruses at 1:160 to 1:320 dilutions and HTN at 1:20 to 1:40 dilutions. The anti-AMR serum neutralized homologous viruses at a 1:80 dilution and HTN at a 1:40 dilution. The anti-HTN serum did not neutralize AMR (<1:40 dilution), although it had a high neutralizing titer (1:320) against the homologous virus. Therefore, we suggest that AMR virus may constitute a distinct serotype within the genus *Hantavirus*.

Keywords: Bunyaviridae; Hantavirus; Hantavirus infections; Hemorrhagic fever with renal syndrome; Hantaan; Amur

Hantavirus, which is a member of the genus *Hantavirus* of the family Bunyaviridae, is enveloped, and contains tripartite, single-stranded, negative-sense RNA segments. The small (S), medium (M), and large (L), RNA segments encode a nucleocapsid protein (NP), surface glycoproteins G1 and G2, and the viral polymerase, respectively (Antic et al., 1991; Schmaljohn and Dalrymple, 1983; Hung et al., 1983; Plyusnin et al., 1996). It has been shown that the hantavirus NP acts as the major cross-reactive antigen between the different antigenic groups of hantaviruses (Sheshberadaran et al., 1988). The hantavirus G1 and G2 proteins mediate many important biological properties, such as virulence, neutralization, hemagglutination, and cell fusion (Elliot, 1990). Studies on the antigenic characterization of the Hantaan (HTN) virus envelope glycoproteins have shown that the G1 and G2 proteins contain major antigenic determinants that play an important roles in the induction of protective humoral immunity to hantavirus infection (Arikawa et al., 1989; Dantas et al., 1986; Lundkvist and Niklasson, 1992; Ruo et al., 1991). The deduced amino acid sequences of certain hantaviruses have shown that the L proteins are more conserved than the gene products of the M or S segment (Antic et al., 1991; Schmaljohn, 1990; Stohwasser et al., 1991).

Some hantaviruses cause severe human illnesses, such as the hemorrhagic fever with renal syndrome (HFRS) that is endemic to Eurasia, and the hantavirus pulmonary syndrome (HPS) that is endemic to the Americas (CDC, 1993; Clement et al., 1997; Hughes et al., 1993). It is well known that hantaviruses are transmitted to humans via infectious aerosols from persistently infected rodents (Tsai, 1987) or via contaminated saliva in animal bites (Douron et al., 1984). Thus, both HFRS and HPS are considered important rodent-borne zoonoses (Lee and Van der Groen, 1989; Nichol et al., 1993; Zaki et al., 1995).

* Corresponding author. Tel.: +81-11-706-5212; fax: +81-11-706-5213.
E-mail address: kariwa@vetmed.hokudai.ac.jp (H. Kariwa).

0168-1702/$ – see front matter © 2004 Elsevier B.V. All rights reserved.
doi:10.1016/j.virusres.2003.12.031

The HTN and Seoul (SEO) viruses cause HFRS in Asia (Lee et al., 1978; Kitamura et al., 1983), and represent a considerable public health problem in China with almost 100,000 cases reported annually (Lee, 1996; Song, 1999). Recent studies have revealed that the HTN and SEO viruses in China are carried by *Apodemus agrarius* and *Rattus norvegicus*, respectively, and these viruses are the major causes of HFRS (Song et al., 1984; Kariwa et al., 2001). Many hantaviruses have been isolated from various rodent species and patients in China. These isolates were found to be antigenically related to HTN or SEO (Tang et al., 1991; Liang et al., 1994). Furthermore, a distinct novel hantavirus type, NC167, has been isolated recently from *Niviventer confucianus*. Nucleotide and amino acid comparisons confirm that NC167 represents a novel hantavirus type, which have been named provisional "Da Bie Shan virus". In addition, a new subtype of SEO virus, Gou3, has been isolated from *Rattus rattus* (Wang et al., 2000).

Far East Russia is an endemic area for the clinically severe form of HFRS, and many different hantaviruses have been found in various rodent species and in patients in this area (Kariwa et al., 1999). Recently, two hantavirus lineages, which have been designated Amur (AMR) and Far East (FE), were identified in severe HFRS patients in the same area (Yashina et al., 2000; Miyamoto et al., 2003). It has been revealed that *A. peninsula* is the reservoir animal for the AMR lineage (Yashina et al., 2001; Lokugamage et al., 2002). These lineage viruses appear to be related to HTN viruses but show divergence, according to limited sequence analyses. Although the AMR and FE lineages cause severe HFRS in humans, the genetic and antigenic properties of these lineages have not been characterized adequately. Our previous findings suggest a variety of lineages among the HTN-related viruses in China, and indicate that viruses that are closely related to AMR and FE also exist in China (Wang et al., 2000; Lokugamage et al., 2002). Phylogenetic analysis, based on partial M gene nucleotide sequences, suggests that two Chinese human isolates, H5 and B78, belong to the AMR lineage, while another Chinese isolate from *A. agrarius*, Bao 14, belongs to the FE lineage. Therefore, we used these isolates to elucidate the genetic and antigenic properties of AMR and FE lineages, which are related to, but show genetic divergence from, the HTN virus.

The hantaviruses used in this study were propagated in Vero E6 cells that were cultivated in Eagle's minimal essential medium (MEM; Nissui, Tokyo, Japan) supplemented with 5% fetal calf serum, kanamycin and L-glutamine. All viruses used in this study were handled in a biosafety level 3 laboratory. The Hantaan 76-118 and SR-11 strains were used as prototypes of the HTN and SEO viruses, respectively. The three Chinese isolates (H5, B78, and Bao14) examined in this study were kindly provided by Dr. C. Hung of the Chinese Academy of Preventive Medicine. H5 and B78 were isolated from HFRS patients, while Bao 14 was isolated from *A. agrarius*.

Five-week-old specific-pathogen-free male ICR mice (SLC, Hamamatsu, Japan) were inoculated subcutaneously (sc) with 1×10^2–1.6×10^3 FFU of HTN 76-118, SR-11, H5, B78, and Bao14, and were supplied with food and water ad libitum. The mice were bled for immune sera 2 months later by cardiac puncture under anesthesia. All of the animal experiments were carried out in biosafety level 3 facilities according to the guidelines for animal experimentation of the Graduate School of Veterinary Medicine, Hokkaido University.

The Vero E6 cells were infected with viruses and spotted onto 24-well slides. After incubation at 37 °C for 4 h, the slides were fixed with cold acetone. The air-dried slides were used as antigen slides. A panel of monoclonal antibodies (MAbs) that recognize glycoproteins G1 and G2, and the nucleocapsid protein of HTN or SEO virus was used in a standard IFA on acetone-fixed, H5, B78, Bao 14, HTN 76-118, and SR-11 infected Vero E6 cells (Arikawa et al., 1989; Yoshimatsu et al., 1996). Briefly, serially diluted Mabs (1:1 to 1:1000 for MAbs that were derived from culture supernatant and 1:100 to 1:100,000 for Mabs that were derived from ascitic fluids) were spotted onto infected Vero E6 cells and incubated for 1 h at 37 °C. After three washes with phosphate-buffered saline (PBS), fluorescein isothiocynate (FITC)-conjugated antibody to mouse IgG was added to the cells (ICN pharmaceuticals Inc., Aurora, OH). Incubation at 37 °C for 1 h was followed by three washes with PBS. Specific antibody binding was detected by fluorescent microscope.

The endpoint titers of the neutralizing antibodies were determined by FRNT. Mouse immune sera, which were prepared against H5, B78, Bao14, HTN 76-118, and SR-11 viruses, were used to analyze the serological relationships among AMR and FE genotypes and the HTN virus. Serially diluted antisera (100 μl) were mixed with equal volume of the stock viruses (100 focus-forming units/100 μl). After 1 h incubation at 37 °C the mixtures (100 μl/well) were inoculated onto Vero E6 cells monolayers that were grown in eight-well slides. After adsorption for 1 h at 37 °C, the inocula were removed and MEM that contained 1.5% carboxymethyl cellulose (CMC) was layered onto the cells. The slides were incubated in a CO_2 incubator at 37 °C for 5–7 days. After this incubation period, the monolayers were washed with PBS, fixed with cold acetone, and air-dried. Mouse immune sera to the HTN virus were added to the fixed Vero E6 cells. Incubation for 1 h at 37 °C was followed by three washes with PBS. The FITC-conjugated antibody to mouse IgG was added to the cells and incubated at 37 °C for 1 h. FITC-stained foci were counted under a fluorescence microscope. The FRNT titer was determined as the highest dilution of the serum that showed 80% or higher reduction of focus formation.

Total cellular RNA was extracted from the virus-infected Vero E6 cells using Isogen (Nippon Gene Co. Ltd., Osaka, Japan) according to the manufacturer's instructions. Reverse transcription was carried out at 42 °C for 30 min with

superscript II and Random primers (Gibco-BRL, Rockville, MD). The amplification of the S and M segments was similar to the method described previously (Lokugamage et al., 2002). Totally 32 primers were used for amplification or sequencing the S and M segments. The amplified segments were sequenced directly using a Big Dye terminator (Applied Biosystems, Lincoln Centre Drive, Foster City, CA, USA) and an ABI 310 genetic analyzer.

The CLUSTALX program package (Version 1.81;URL: ftp://ftp-igbmc.u-strasbg.fr/pub/clustalx) was used to generate the phylogenetic tree using the neighbor-joining method with 1000 bootstrap replicates. The hantavirus sequences used in the comparisons were obtained from GenBank.

In our previous study, limited sequencing analysis suggested the existence in China of viruses that are closely related to the AMR and FE lineages (Lokugamage et al., 2002). Although the sequences of the AMR and FE lineages have been identified in HFRS patients, and these lineages may be the major cause of the disease in Far East Russia, the characterization of these viruses has not been defined precisely and has been limited to the analysis of partial gene sequences. Therefore, the information needed to classify these viruses has been lacking. In addition, these viruses appear to exist in a vast area of the Eurasian continent, including Far East Russia, China, and Korea, and they cause a number of HFRS cases. Therefore, we sequenced the G2 regions on the M segments of these three Chinese isolates and performed phylogenetic analyses (Fig. 1). The phylogenetic tree clearly shows that H5 and B78 belong to the AMR lineage, which includes sequences derived from HFRS patients and

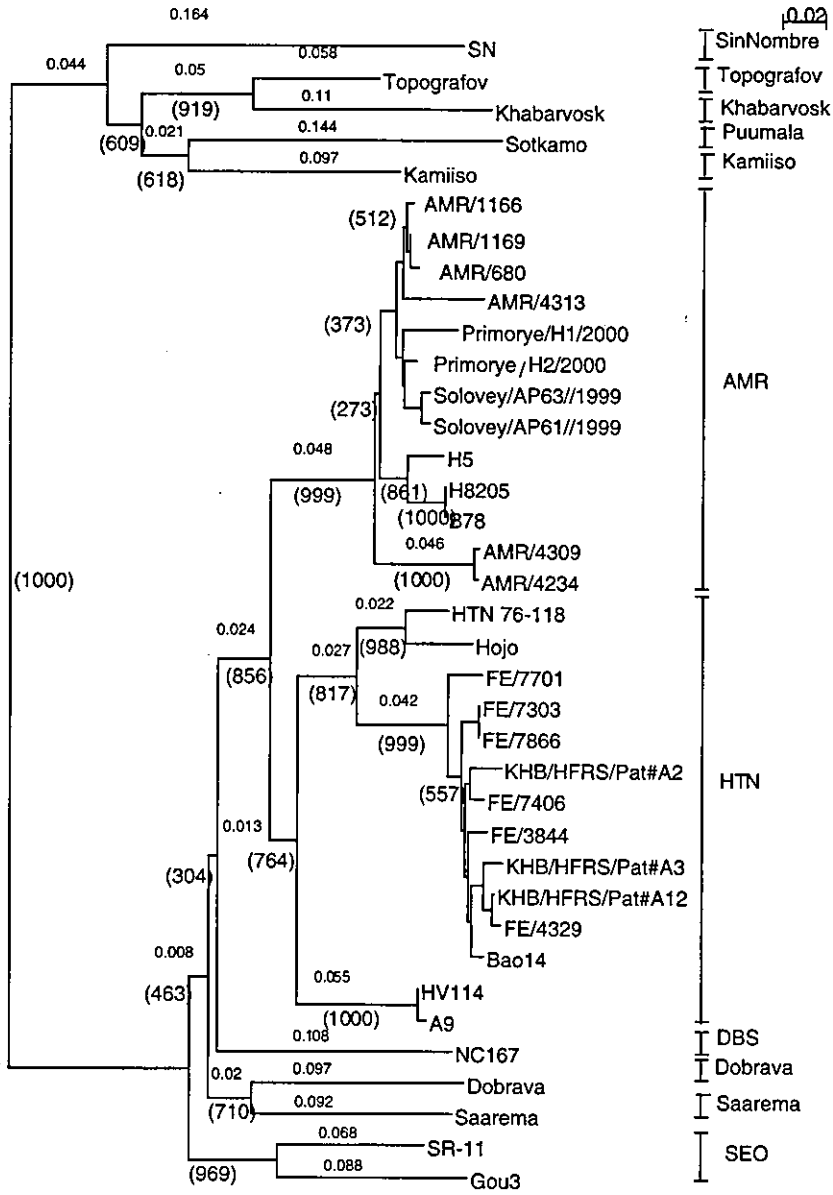

Fig. 1. Phylogenetic tree of the hantavirus partial M (nt 2736–2968) segments. The tree was constructed using the CLUTALX (Version 1.81) program. The numbers above the branches are the distances and those in parentheses are the bootstrap support values for 1000 replicates.

A. peninsulae. In contrast, Bao 14 belongs to the FE lineage, which includes sequences from HFRS patients.

To reveal detailed genetic information on the AMR and FE lineages, we amplified and sequenced the entire S segments of the H5, B78, and Bao 14 strains, except for the 20 nucleotides at the 3′- and 5′-ends (AB127996, AB127997, and AB127998). The nucleotide and amino acid identities among the AMR lineage (H5, B78, and SL/AP/63) were 90.9–99.8 and 98.6–100%, respectively. The AMR lineage and Bao 14 had 85.2–86.0 and 97.2–97.7% identities at the nucleotide and amino acid levels, respectively. The S gene of AMR lineage had diversities, at 16–17 and 3–4% in nucleotide and amino acid levels, respectively, with the prototype HTN virus. Meanwhile, the S gene of FE lineage differed by only 10 and 0.9% difference in nucleotide and amino acid levels, respectively, with the prototype HTN virus.

To provide further insight into the genetic relationship between the AMR- and FE-lineage viruses, the entire M segments of H5, B78, and Bao 14 (AB127993, AB127994, and AB127995) were sequenced and compared. The nucleotide and amino acid identities among the AMR lineage (H5, B78, and H8205) were 96.3–99.5 and 98.5–99.2%, respectively. The nucleotide and amino acid identities between AMR and the other HTN-related viruses (A9, Bao14, HTN 76-118, Lee, and Hojo) were approximately 80 and 91–92%, respectively. Bao 14 had 87.8 and 97.9% identities

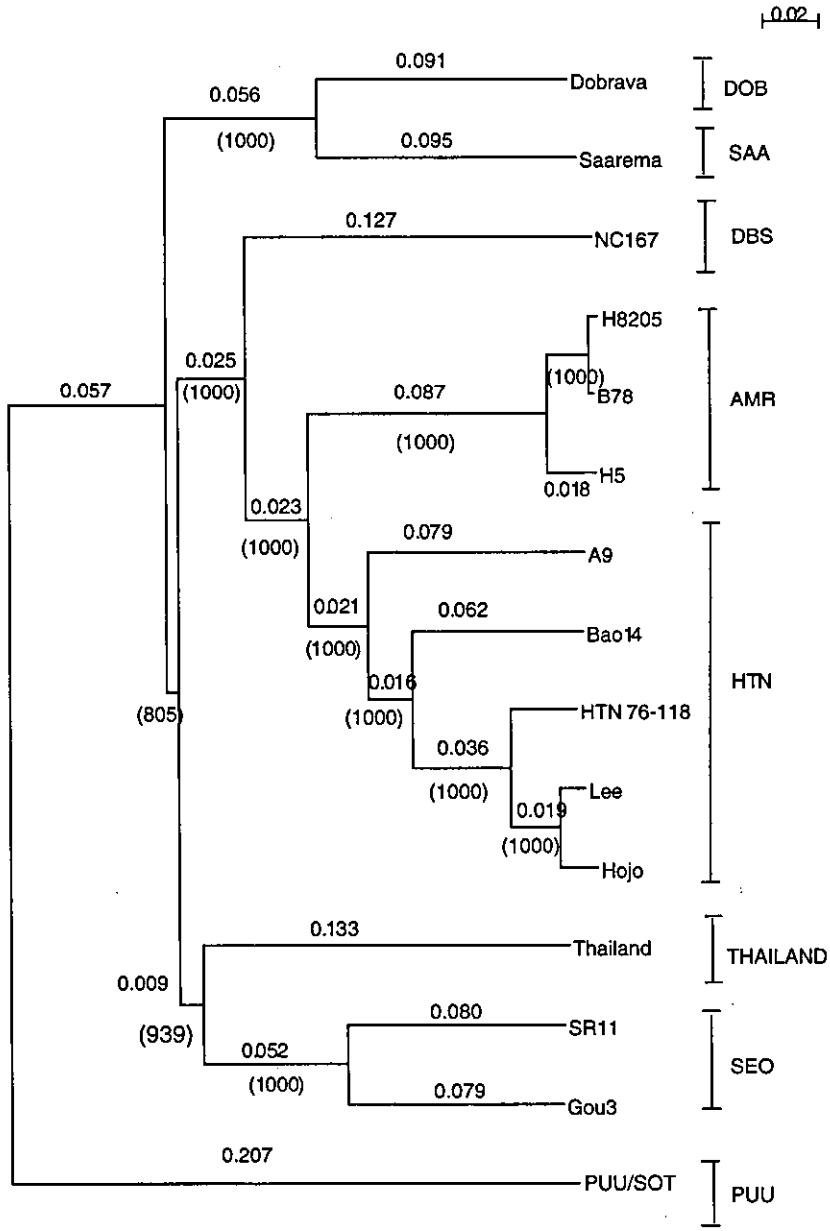

Fig. 2. Phylogenetic tree of the hantavirus entire M segments except for 20 nucleotides at both ends. The tree was constructed using the CLUTALX (Version 1.81) program. The numbers above the branches are the distances and those in parentheses are the bootstrap support values for 1000 replicates.

with HTN 76-118 at the nucleotide and amino acid levels, respectively.

The phylogenetic tree on the complete M segments showed that the H5 and B78 viruses formed a single cluster, together with H8205, which is one of AMR viruses, with high bootstrap support values. It was also clear that Bao 14 virus was monophyletic with the HTN virus (Fig. 2). These results indicate the AMR lineage viruses may form a distinct branch from the HTN clade but the FE may be the subtype of the HTN virus.

Ten out of fourteen amino acid mutations in the S segments of the aligned sequences were unique to the AMR-lineage viruses (data not shown). With respect to the amino acid alignment of the glycoprotein precursor (GPC), six possible asparagine-linked glycosylation sites on GPC were totally conserved in the AMR, FE, and HTN viruses (Fig. 3). In our previous study, we identified signature amino acids for AMR lineage that was based on the deduced partial amino acid sequences of GPC. The present data show that these signature amino acids are present in deduced

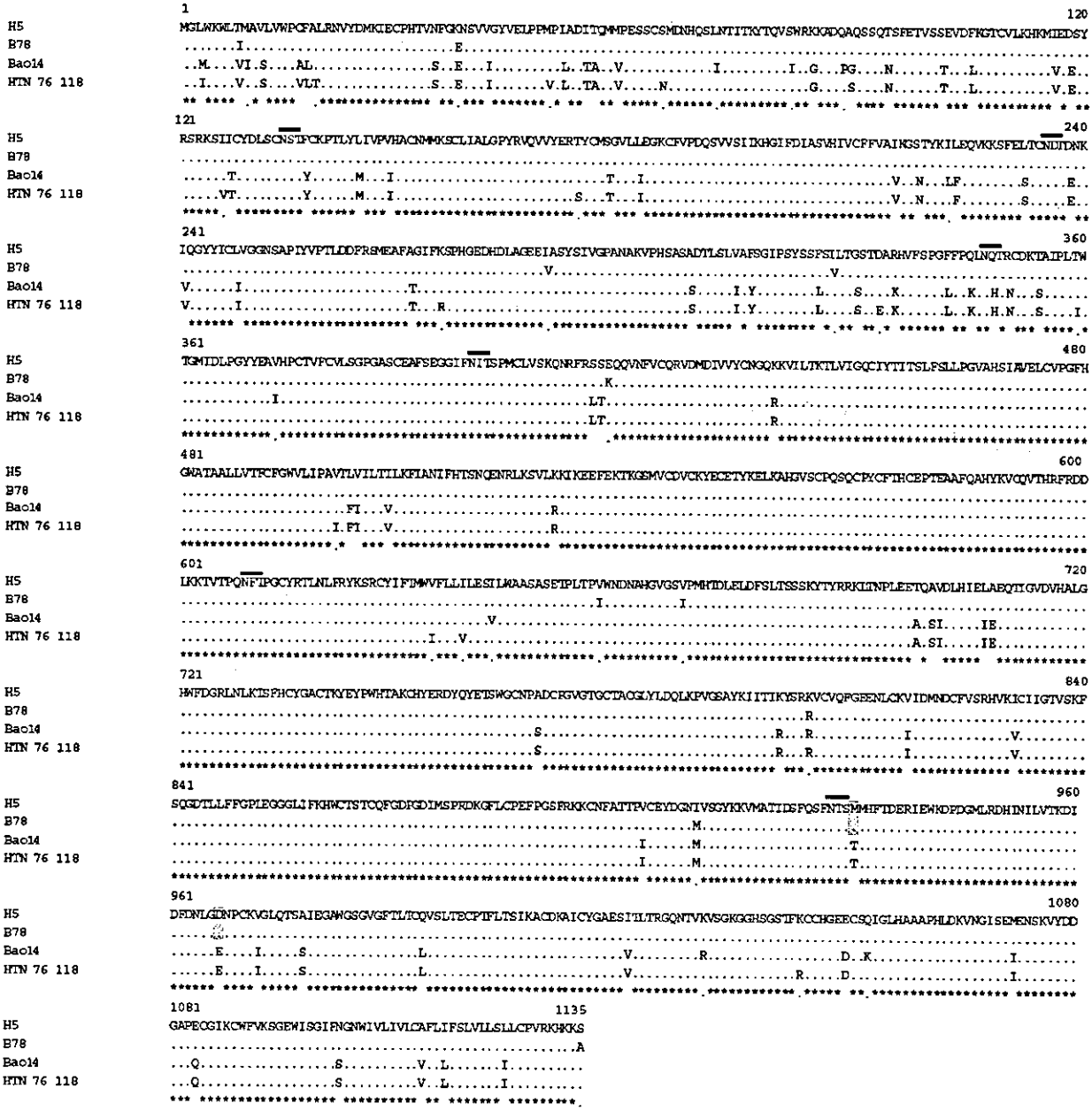

Fig. 3. Multiple alignment of the deduced amino acid sequences of the G1 and G2 regions of hantaviruses. The amino acid sequences were analyzed using the CLUTALX (Version 1.8) program. The amino acid positions indicated above the sequences are based on those of HTN 76-118. The first line shows the deduced amino acid of H5. The dots represent amino acids that are identical to those at corresponding positions in the H5 sequence. Amino acids that differ from those in the H5 sequence are indicated at the relevant positions. The signature amino acids for AMR sequences, which were identified in our previous study, are shaded. Possible asparagine-linked glycoprotein sites are indicated by lines over the corresponding sites.

Table 1
Antigenic characterization of HTN 76-118, Bao 14, H5, B78, and SR-11 by a panel of monoclonal antibodies

Virus	Antigenic site	Mab	HTN 76-118	Bao14	H5	B78	SR 11
HTN	G1-a	6D4	+	+	+	+	−
		10 F 11	+	++	+	+	−
	G1-b	16D2/3D5	+	+	+	+	−
		2D5	+	+	−	−	−
	G2-a	HCO2	++	+	++	++	+
		16E 6	++	+	+	+	−
	G2-b	EBO6	+	+	+	+	+
	G2-c	11 E 10 2-2	++	++	++	++	−
	G2-d	17G6	+	+	+	+	+
		3D7	++	++	+	+	+
		5 B 7	+	+	++	+	+
	G2-e	20 D 3	+	++	+	+	+
	G2-f	8 E 10/ 23G 10-1/18 F 5/1 C 6	+	+	+	+	+
		7G6/1 G 6	+	++	++	+	+
		3 B 6	+	+	+	+	++
		1G8	++	++	++	+	+
	NP-I	ECO2	++	++	++	++	+
	NP-III	C16D11	++	++	++	++	+
		C24B4	++	++	++	++	−
		F23A1	++	++	+	+	+
SEO	NP	2 E 8	−	−	−	−	++

Antibody reactivity is defined as: −, <10; +, 10–100; ++, 1000.

amino acid sequences of H5 and B78, which confirm that these two strains belong to the AMR lineage.

The antigenic characterization of the AMR and FE lineages was performed with a panel of MAb to glycoproteins G1 or G2 and NP (Table 1). Almost all MAb used in this study were reacted with the HTN, AMR, and FE viruses with more or less in similar patterns, except for the 2D5 MAb, which recognizes G1-b site. This particular MAb did not react with the H5 and B78 viruses, which implies that these viruses contain amino acid changes in the epitope for this MAb.

However, cross-neutralization analysis showed that the AMR lineage viruses had apparently distinct antigenicities as compared to that of the prototype HTN virus (Table 2). The titers of the anti-H5 and anti-B78 sera to homologous viruses (1:80) were two-fold higher than that against the HTN virus (1:40), while the titer of anti-HTN immune serum to the homologous HTN virus (1:320) was eight-fold higher than that against the H5 and B78 viruses (<1:40). In addition, when we used sera from two *A. peninsulae* which were captured in the suburb of Vladivostock and which had AMR sequences (SL/AP61/2000 and SL/AP63/2000) in their lungs (Lokugamage et al., 2002), the titers of those two sera to the H5 and B78 viruses (1:160 to 1:320) were eight-fold higher than those against the HTN virus (1:20 to 1:40). Furthermore, the titer of anti-Bao 14 to the homologous virus (1:1280) was 16–32-fold higher than those against the AMR lineage viruses (1:40 to 1:80) but was

Table 2
Antigenic characterization by cross focus reduction neutralization test

Antisera	Species	Neutralization titer to the following viruses[a] H5	B78	Bao14	HTN 76-118	SR-11
H5	Mouse	80[b]	80	80	40	<40
B78	Mouse	80	80	160	40	<40
#61[c]	*A. peninsulae*	160	320	20	20	ND[d]
#63[c]	*A. peninsulae*	320	320	40	40	ND
Bao14	Mouse	40	80	1280	320	40
HTN 76–118	Mouse	<40	<40	320	320	<40
SR-11	Rabbit	10	<10	<10	10	160

[a] Neutralization titer was expressed as a reciprocal of the highest dilution which showed 80% or more of inhibition of the virus focus formation.
[b] Neutralization titer with homologous immune sera was underlined.
[c] Sera from *Apodemus peninsulae* which were captured in the suburb of Vladivostock and had Amur sequences in their lungs (34).
[d] Not done.

four-fold higher than that against the HTN virus. These results indicate that the H5 and B78 viruses are antigenically distinguishable from HTN virus with a four-fold titer difference in two-way cross-neutralization. Further, the anti-HTN immune serum titer to the homologous HTN virus (1:320) was similar to that of Bao 14 virus (1:320) (Table 2).

The three-dimensional neutralizing epitope in AMR lineage viruses may differ from that in the HTN virus. This finding is important, as the hantavirus vaccine strains that have been developed in China and Korea are closely related to the prototype of HTN virus. Thus, these vaccines may not protect against infection with AMR lineage viruses.

Hantavirus classification is very complicated because of the geographic variation among hantaviruses that are carried by single or several closely related host species. Elliot et al. (1999) suggested the following criteria for the distinction of viruses in the genus *Hantavirus*: (a) a unique ecological niche for each virus species, i.e., a clear association of a new hantavirus with a different primary rodent reservoir species or subspecies; (b) at least 7% amino acid sequence difference from previously characterized hantaviruses (on comparison of the complete glycoprotein precursor and nucleocapsid protein sequences); (c) at least a four-fold difference in two-way cross-neutralization tests; (d) absence of genetic reassortment in nature.

Accordingly, the AMR lineage viruses are carried by *A. peninsulae* not by *A. agrarius* (Lokugamage et al., 2002). Furthermore, the amino acid diversity of the glycoprotein precursor is more than 7% as compared to other HTN viruses. In addition, the difference in neutralizing titer is greater than eight-folds in two-way cross-neutralization tests. There is no information about re-assortmants between the AMR and other hantaviruses. Therefore, AMR meets most of the criteria for a distinct virus. In contrast, the FE viruses do not meet these criteria.